Nodal secures pluripotency upon embryonic stem cell progression from the ground state

Carla Mulas[1], Tüzer Kalkan[1], Austin Smith[1,2,*]

[1]Wellcome Trust – Medical Research Council Stem Cell Institute, University of Cambridge, Tennis Court Road, CB2 1QR, Cambridge, UK

[2]Department of Biochemistry, University of Cambridge, Tennis Court Road, CB2 1GA, Cambridge, UK

*Correspondence: austin.smith@cscr.cam.ac.uk

Running title (50 characters):

Nodal capacitates pluripotency

SUMMARY (150 words)

Naïve mouse embryonic stem (ES) cells can readily acquire specific fates, but the cellular and molecular processes that enable lineage specification are poorly characterised. Here we investigated progression from the ES cell ground state in adherent culture. We utilised down-regulation of *Rex1::GFPd2* to track loss of ES cell identity. We found that cells that have newly down-regulated this reporter have acquired competence for germline induction. They can also be efficiently specified for different somatic lineages, responding more rapidly than naïve cells to inductive cues. Nodal is a candidate autocrine regulator of pluripotency. Abrogation of Nodal signalling did not substantially alter kinetics of exit from the ES cell state, but accelerated subsequent adoption of neural fate at the expense of other lineages. This effect was evident if Nodal was inhibited prior to extinction of ES cell identity. We suggest that Nodal is pivotal for non-neural competence in cells departing naïve pluripotency.

INTRODUCTION

Pluripotency denotes a flexible cellular potential to differentiate into all lineages of the developing embryo. This property emerges in the epiblast of the pre-implantation blastocyst (Boroviak et al., 2014; Gardner, 1975; Rossant, 1975). After implantation, epiblast cells remain pluripotent while undergoing profound cellular and molecular changes in preparation for gastrulation (Smith, *in press*). In mice the post-implantation epiblast develops into a cup-shaped epithelium, the egg cylinder. Signalling cues from extra-embryonic tissues then pattern the egg cylinder to establish anterior-posterior and proximal-distal axes prior to lineage specification (Arnold and Robertson, 2009; Beddington and Robertson, 1998; Peng et al., 2016; Rossant and Tam, 2009; Thomas and Beddington, 1996).

In mouse the naive phase of pluripotency can be captured in culture in the form of embryonic stem (ES) cells (reviewed by Nichols and Smith, 2012). Dual inhibition (2i) of Mek1/2 and GSK3, in optional combination with the cytokine Leukemia Inhibitory Factor (LIF), allows mouse ES cells to maintain the transcription profile, DNA methylation status and developmental potential characteristic of the pre-implantation epiblast from which they are derived (Boroviak et al., 2014; 2015; Habibi et al., 2013; Leitch et al., 2013; Ying et al., 2008). ES cells in 2i are stable and relatively homogeneous, a condition referred to as “ground state” (Marks et al., 2012; Wray et al., 2010). Such uniformity in defined conditions provides an experimental system to characterise cellular and molecular events that generate multiple lineage-committed states from a developmental blank canvas.

ES cell progression from the ground state is initiated simply by removal of the inhibitors. In adherent culture this results predominantly in neural specification (Ying et

al., 2003) or in a mixture of neural and mesoendodermal fates, depending on cell density (Kalkan et al., 2016). Previous studies have identified expression of Rex1 (gene name *Zfp42*) as a marker of undifferentiated ES cells (Betschinger et al., 2013; Kalkan and Smith, 2014; Leeb et al., 2014; Toyooka et al., 2008; Wray et al., 2010; 2011; Yang et al., 2012). In this study, we exploit a *Rex1::GFPd2 (RGd2)* reporter cell line (Kalkan et al., 2016) to isolate cells at initial stages of progression from naïve pluripotency following release from 2i in adherent serum-free culture. We examine whether cells exiting the ES cell state guided by autocrine cues commit preferentially to a neural fate or exhibit competence for multilineage differentiation.

RESULTS

Multi-lineage differentiation capacity is retained after loss of naïve ES cell identity

In *Rex1::GFPd2* (RGd2) reporter ES cells, a short half-life GFP is expressed from the endogenous Rex1 (*Zfp42*) locus (Marks et al., 2012; Wray et al., 2011). Loss of the reporter coincides with downregulation of naïve pluripotency factors and functionally with extinction of clonal self-renewal capacity (Kalkan et al., 2016) (Figure S1A-D). GFP downregulation is asynchronous across the population. For at least 16 hours cell remain uniformly GFP positive (Kalkan et al., 2016). By 24hrs, however, GFP is expressed at variable levels and in a minority of cells the reporter is no longer detectable. These Rex1-negative cells have lost the capacity to resume self-renewal in 2i/LIF, whereas cells with high GFP retain comparable colony forming efficiency to cells

taken directly from 2i (Figure S1C). We focussed attention on the character of cells 24hrs after 2i withdrawal, the first time point at which it is practical to isolate a substantial population of Rex1-negative cells by flow cytometry (Kalkan et al, 2016).

We first investigated capacity to form primordial germ cell-like cells (PGCLC). Previous studies have shown that undifferentiated ES cells are not directly competent for germline specification but must first transition to a transient epiblast-like (EpiLC) population which can then be induced to form PGCLC (Hayashi et al., 2011; Nakaki et al., 2013). The EpiLC population is obtained by transfer from 2i/LIF to N2B27 medium supplemented with ActivinA, bFGF and the serum substitute KSR for 48hrs (Hayashi et al., 2011). We assessed whether the first cells that exit the ground state in N2B27 alone exhibit competence to form PGCLC. For this purpose we used RGd2 ES cells transfected with a doxycycline (Dox)-regulatable expression construct containing the three germ line determination factors *Prdm1* (Blimp1), *Prdm14* and *Tfap2c* (Magnúsdóttir et al., 2012; Nakaki et al., 2013). Stable transfectants were withdrawn from 2i for 24hrs and the high and low GFP fractions isolated by fluorescence-activated cell sorting (FACS) (Figure 1A). For each fraction, 3000 cells were aggregated in non-adherent 96 well plates in medium containing 15% KSR with or without Dox (Nakaki et al., 2013). After 4 days, few cells co-expressing Blimp1 with Oct4 were present in aggregates from either population without Dox. Dox treatment did not increase the frequency of co-expression from Rex1-positive cells, but induced many double positive cells from the Rex1-negative fraction (Figure 1B and C). Dual expression of Blimp1 and Oct4 is a combination unique to PGCs and PGCLCs (Hayashi et al., 2011; Kurimoto et al., 2008; Nakaki et al., 2013). Furthermore, undifferentiated ES cells do not tolerate appreciable levels of Blimp1 protein (Magnúsdóttir et al., 2013). Quantitative image

105 analysis confirmed more intense Blimp1 staining in cultures derived from Rex1-negative
106 cells (Figure 1D). By RT-qPCR analysis we detected upregulated expression of
107 endogenous *Prdm1* (Blimp1), along with *Prdm14*, *Tfap2c*, *Nanos3* and *Stella*, as well as
108 maintenance of *Pou5f1* (Oct4) (Figure 1E). *T* (Bra) was induced transiently on day 2 as
109 previously described for PGCLC induction (Figure 1E) (Nakaki et al., 2013). Thus ES
110 cells that have newly exited the ground state under autocrine stimulation in defined
111 conditions acquire competence for germline specification.

112 We then examined somatic lineage potential of Rex1-negative cells. Sorted fractions
113 were plated in media that favour mesoderm, definitive endoderm or neural lineages
114 respectively and the timing and efficiency of differentiation quantified.

115 ActivinA combined with GSK3 inhibition (GSK3(i)), elicits the upregulation of
116 primitive-streak markers such as T (Tbra) in differentiating ES cells (Gadue et al., 2006;
117 Tsakiridis et al., 2014; Turner et al., 2014)Morrison et al., 2015). We modified *RGd2*
118 cells to express an mKO2 fluorescent reporter from the *T(Bra)* locus (Figure 2A).
119 *T::mKO2* was not expressed in undifferentiated ES cells in 2i (Figure S2A), and not
120 detected until day 3 of treatment with Activin plus GSK3(i). In contrast, Rex1-negative
121 cells replated in the presence of ActivinA and GSK3(i) upregulated *T::mKO2* after one
122 day and all cells were positive by day 2. Rex1-positive cells upregulated *T::mKO2* at an
123 intermediate rate and some cells remained GFP-positive even after 3 days, indicating
124 they remained undifferentiated and unresponsive to differentiation cues (Figure 2B). To
125 test further mesoderm differentiation, we plated the sorted fractions in conditions that
126 promote lateral mesoderm (Nishikawa et al., 1998; Yamashita et al., 2000). All
127 populations gave rise to Flk1 positive/E-cadherin negative cells after 4-5 days (Figure
128 2C).

Differentiation into definitive endoderm was assessed by monitoring the percentage of Cxcr4/E-cadherin double positive cells (Morrison et al., 2008; Yasunaga et al., 2005) under inductive conditions applied after sorting (Morrison et al., 2015)(Figure 2D). Compared to 2i cells or the Rex1-positive population, a lower proportion of Rex1-negative cells upregulated Cxcr4 (Figure 2E). However, we observed that the majority of Rex1-negative cells died after replating in these conditions (Figure 2F). The survivors could form Sox17/Foxa2 double positive cells, although with lower efficiency than 2i or Rex1-positive cells (Figure S2B). Every Sox17 positive cell was also positive for Foxa2, substantiating endoderm identity (Burtscher and Lickert, 2009). Acquisition of the later marker, Sox17, was specifically reduced in the Rex1-negative cells. We hypothesised that Rex1-negative cells might display impaired survival and differentiation because of a requirement for high cell density and cell-cell contact for the endoderm programme. We therefore combined sorted cells with unsorted populations to reproduce the density of non-manipulated cultures (Figure 2G). To trace the sorted cell progeny we employed *RGd2* cells constitutively labelled with mKO2 under the control of a CAG promoter (Niwa et al., 1991). Two hundred sorted labelled cells were plated together with $5.8x10^3$ parental cells per $3.8cm^2$ dish. Cells were exposed to definitive endoderm differentiation media then fixed and stained for Sox17 at day 4. The total number of mKO2 positive clones was determined, as well as the number of Sox17 positive cells per clone and clone sizes using CellProfiler (Jones et al., 2008). Slightly fewer clones were obtained from Rex1-negative cells (Figure 2H, Student t-test $p<0.05$) and their distribution was skewed towards smaller colonies (Figure 2I, two-sample Kolmogorov-Smirnov test $p<0.001$), with more Sox17 negative cells per colony (Figure 2J, two-sample Kolmogorov-Smirnov test $p<0.01$). These differences were modest however.

153 Importantly, the majority of Rex1-negative cells were able to produce colonies
154 containing Sox17 positive cells.

155 Finally, we examined cell fate acquisition in N2B27 alone, which is permissive for
156 neural differentiation (Ying et al., 2003). The great majority (≤80%) of cells from both
157 Rex1 fractions became immunopositive for Sox1, an exclusive marker of neurectoderm
158 (Pevny et al., 1998; Zhang et al., 2010) (Figure 2K). However, Rex1-negative cells
159 showed earlier upregulation of Sox1, with most cells becoming Sox1 positive on day 2,
160 a day before the Rex1-positive population (Figure 2K). Cell viability and expansion were
161 not significantly different between the populations (Figure S2C). Rex1-negative cells
162 subsequently also showed accelerated onset of expression of the neuronal marker type
163 III β −tubulin (Lee et al., 1990)(Figure S2D).

164 Overall, these data indicate that after 24hrs of monolayer differentiation guided by
165 autocrine cues, cells in the Rex1-negative population are poised for multilineage
166 specification and respond more rapidly to induction than either ground state ES cells or
167 Rex1-positive cells.

168

169 **Nodal does not regulate kinetics of exit from the naïve state**

170 FGF4 is a known autocrine factor that drives ES cell transition upon release from 2i
171 (Betschinger et al., 2013; Kunath et al., 2007; Leeb et al., 2014; Stavridis et al., 2007). A
172 second potential autocrine regulator is Nodal (Fiorenzano et al., 2016; Mullen et al.,
173 2011; Ogawa et al., 2007). Detection of Smad2 phosphorylation indicates that
174 endogenous Nodal/TGFβ signalling is active in ES cells in 2i (Figure S3A). Treatment
175 with the Alk5/4/7 receptor inhibitor A83-01 (Alk(i)) (Tojo et al., 2005) eliminated Smad2
176 phosphorylation after 30 minutes (Figure S3A). However, culture in Alk(i) did not affect

177 colony forming capacity in 2i/LIF, even after continuous culture for three passages
178 (Figure S3B), confirming that Nodal plays little or no role in maintenance of ground state
179 mouse ES cells.

180 We examined the contribution of autocrine Nodal signalling in progression from the
181 ES cell state. We analysed changes in gene expression in cells withdrawn from 2i in the
182 continuous presence of Alk(i) and found no difference in the dynamics of
183 downregulation of *Nanog* or *Klf2* mRNA (Figure 3B), nor of Nanog and Klf4 protein
184 (Figure 3C). The rate of decay in ES cell clonogenicity was also unaffected (Figure 3D).
185 We conclude that Nodal signalling does not promote initial exit from the naïve state.

186 We examined expression of genes associated with the early post-implantation
187 epiblast. Initial upregulation of pan-epiblast genes *Fgf5* and *Otx2* was not significantly
188 altered when Nodal signalling was inhibited (Figure 4E). However, these genes were
189 subsequently downregulated more abruptly on day 3/4 (Figure 4E). Conversely,
190 transcripts for neuroectodermal lineage factors *Sox1*, *Zic1* and *Pou3f3* were strongly up-
191 regulated in day 3/4 Alk(i) treated cultures, before appreciable expression in vehicle
192 treated cells (Figure 3F). At the protein level, most cells in Alk(i) treated cultures had
193 downregulated Oct4 and were Sox1 positive after 3 days, indicative of neural
194 commitment, whereas control cultures displayed a mosaic pattern of co-exclusive Sox1
195 and Oct4 immunostaining (Lowell, 2006) (Figure 3G).

196 To validate findings with the inhibitor we deployed siRNAs against Nodal signalling
197 pathway components. In *Nodal, Smad2/3* and *Tdgf1* knockdown experiments the
198 emergence of Oct4-/Sox2+ and Sox2+/Sox1+ cells was accelerated (Figure S3C-D).
199 We conclude that suppression of Nodal signalling does not substantially affect initial exit
200 from the naïve state but promotes subsequent specification to the neural lineage.

201

202 **Nodal signalling is required to prevent precocious neuralisation and to potentiate**
203 **other lineages**

204 Examination of Nodal signalling components in RNAseq data from *RGd2* sorted cells
205 (Kalkan et al., 2016) revealed that pathway ligands, receptors, intracellular mediators
206 and target genes are expressed in undifferentiated ES cells and in 24hr Rex1 positive
207 cells. Rex1-negative cells, however, display reduced expression of *Nodal*, Nodal
208 proprotein convertase *Pcsk6 (*Pace4*)*, and Nodal signalling pathway targets *Lefty1,*
209 *Lefty2* and *Smad7* (Figure S4A). Consistent with pathway down-regulation in Rex1-
210 negative cells, we found that when cells were exposed to Alk(i) only after sorting, the
211 Rex1-negative fraction showed no change in kinetics of Sox1 acquisition. In contrast the
212 Rex1-positive population responded by accelerated expression at day 2 (Figure 4A,
213 Student t-test $p<0.05$).

214 In light of these results, we postulated that Nodal signalling may function during the
215 primary transition from naïve pluripotency. We therefore inhibited Nodal signalling for
216 only the 24hrs immediately following 2i withdrawal and analysed the resulting Rex1-
217 negative cells (Figure S4B). In line with previous results for continuous treatment,
218 exposure to Alk(i) for 24hrs had little effect on downregulation of Rex1 (Figure S4B) or
219 of naïve pluripotency factor transcripts for *Nanog, Esrrb, Zfp42* (Rex1) and *Klf4* (Figure
220 S4C). Upregulation of early post-implantation markers *Fgf5, Dnmt3b, Otx2* and *Pou3f1*
221 was also similar to vehicle-treated cells (Figure S4C). *Sox1* mRNA was not detected at
222 24hrs, irrespective of the presence of Alk(i) (Figure S4D). Sox1 protein was detectable
223 only in a minority of untreated cells on day 1 after sorting and increased thereafter. In
224 contrast up to half of cells generated after Alk(i)-treatment upregulated Sox1 protein on

day 1 (Figure 4B). This difference does not appear to be due to differential replating efficiency (Figure 4C).

We examined whether faster neural specification as a consequence of Alk(i) pre-treatment has consequences for other lineages. We analysed the response of Alk(i)-treated cells to ActivinA/Gsk3(i). Rex1-negative cells showed a major reduction in the total number of *T::mKO2* positive cells (Figure 4D). Interestingly, this was mainly attributable to reduced cell numbers after exposure to ActivinA/Gsk3(i) (Figure 4E, S4E). A similar reduction in cell survival/proliferation was observed in cells exposed to lateral mesoderm differentiation conditions (Figure S4F-H). To evaluate endodermal specification we employed the clonal mixing protocol described previously (Figure 4F). We observed a shift to fewer Sox17 positive cells per clone (Figure 4G), although the clone sizes (Figure 4H) or total number of clones (Figure S4I) were not reduced in the Alk(i) pre-treated population

Finally, we assessed whether pre-treatment with Alk(i) for 24hrs affected the potential of Rex1-negative cells to respond to PGC-inducing transcription factors (Figure 4I). Alk(i)-treated cells produced less compact and smaller aggregates than control cultures (Figure 4I). The gene expression profile at day 2 and 4 of culture showed lower upregulation of endogenous *Prdm1* (Blimp1), *Prdm14*, *Nanos3* and *Stella*, indicating significantly impaired PGCLC induction.

These findings indicate that suppression of Nodal signalling reduces the capacity of cells exiting the naïve phase of pluripotency to respond productively to inductive cues for mesoderm, endoderm, and germ cell specification.

DISCUSSION

The defined context of ground state ES cell culture provides opportunities for experimentally dissecting the interplay between intrinsic and extrinsic factors that mediate progression through pluripotency. Here we investigated the trajectory of ES cells released from the ground state with minimal extrinsic input. We isolated cells that have lost ES cell identity within 24hrs based on down-regulation of *RGd2*, corroborated functionally by extinction of self-renewal capability (Kalkan et al., 2016). Newly formed Rex1-negative cells exhibited capacity for differentiation into the germline and somatic lineages (Smith, *in press*). The findings further indicate that endogenous Nodal signalling is crucial for the non-neural competence of cells transitioning from naïve pluripotency.

Rex1-negative cells show more rapid upregulation of lineage markers in response to inductive stimuli compared with ground state ES cells or Rex1-positive cells at 24hrs. They have also gained capacity for PGCLC induction. It has previously been established that responsiveness to germ cell induction cues or factors is not manifest in naive ES cells or the pre-implantation epiblast but is a property acquired during developmental progression (Hayashi et al., 2011; Nakaki et al., 2013). We present evidence elsewhere that early Rex1-negative cells show intermediate gene expression features suggesting they are related to the peri-implantation epiblast (Kalkan et al., 2016). We hypothesise that actual competence for germline and somatic lineage specification is acquired during this period (Smith, *in press*). The molecular nature of competence remains unclear but is likely to involve dissolution of naïve pluripotency transcription factor circuitry, reconfiguration of the enhancer landscape, and widespread

epigenome and chromatin modification (Buecker et al., 2014; Choi et al., 2016; Dunn et al., 2014; Zylicz et al., 2015).

Nodal plays pleiotropic roles in the early embryo. Expression can be detected in the inner cell mass and persists throughout the epiblast until axis specification, when it becomes restricted to the proximal posterior region (Conlon et al., 1994; Mesnard et al., 2006). Nodal activity relies on proprotein convertases, Furin and PACE4, produced by the extraembryonic ectoderm (ExE), which cleave and activate pro-Nodal (Beck et al., 2002; Mesnard et al., 2011). *Nodal* deficient embryos show embryonic lethality at E7.5 (Conlon et al., 1994; 1991; Zhou et al., 1993). They fail to specify the anterior visceral endoderm (AVE) (Brennan et al., 2001), a signalling centre essential for the establishment of anterior-posterior (AP) polarity. Nodal mutants also show precocious upregulation of neural markers throughout the egg cylinder and fail to form a primitive streak (Brennan et al., 2001; Camus et al., 2006; Lu and Robertson, 2004). The multiple functions of Nodal and the complex interplay between extraembryonic tissues and the epiblast have complicated precise delineation of its roles in pluripotency progression and lineage specification (Robertson, 2014).

Mouse ES cells express Nodal and have phosphorylated Smad2/3 proteins (Mullen et al., 2011; Ogawa et al., 2004). Inhibition of Nodal signalling enhances Sox1 expression during differentiation (Matulka et al., 2013; Turner et al., 2014). Our results show that inhibition of endogenous Nodal signalling does not affect the downregulation of pluripotency factors when ground state ES cells are released from 2i, consistent with previous findings (Turner et al. 2014). Upregulation of early post-implantation markers is also unaffected. However, suppression of Nodal signalling results in compromised responses to inductive stimuli for mesoderm and endoderm, and in precocious

upregulation of neural markers. Cells also become less responsive to the forced expression of PGC-specific transcription factors.

Importantly, a requirement for Nodal signalling is apparent prior to exit from the ES cell state, while cells are in the reversible Rex1 positive period of transition (Kalkan et al., 2016; Martello and Smith, 2014). Indeed, subsequent to exit Rex1-negative cells in vitro down-regulate Nodal and become dependent on exogenous ligand for non-neural lineage induction, typically achieved by addition of ActivinA. A similar reduction in the expression of *Nodal* and Nodal target genes is seen in E5.75 epiblast explants after removal of the extraembryonic ectoderm (ExE) (Guzman-Ayala et al., 2004; Mesnard et al., 2006), highlighting the paracrine role of ExE in maintaining Nodal signalling in the embryo.

Our findings in the simple monolayer ES cell system are consistent with genetic evidence that Nodal signalling prevents premature neural differentiation in the embryo (Camus et al., 2006). Importantly, however, they also indicate that endogenous Nodal signalling acts during progression from naïve pluripotency to secure non-neural lineage potency. It has been reported that Smad2/3 is recruited by 'master transcription factors' to regulatory loci in a cell type-specific manner (Mullen et al., 2011). In addition, a recent study in human ES cells also suggested that Smad2/3 is able to recruit histone methyltransferases to gene promoters (Bertero et al., 2015). Therefore, non-neural competence could depend upon the presence of Smad2/3 at specific loci during the ES cell transition from naïve pluripotency.

Overall these results are consistent with the proposition that in defined adherent culture, ES cells transit through a formative phase in which they acquire competence for multilineage differentiation, including the germline (Kalkan and Smith, 2014; Smith, *in*

320 *press*). In this phase, cells are expected to respond to inductive signals rapidly and
321 efficiently, as observed for Rex1 negative cells at 24hrs. Furthermore, our findings
322 highlight a pivotal requirement for Nodal signalling in establishing formative
323 pluripotency.
324

EXPERIMENTAL PROCEDURES

Mouse ES cell culture and differentiation

RGd2 ES cells were derived in 2i/LIF from heterozygous embryos (Kalkan et al., 2016). The *RGd2/T:mKO2* cell line was generated by targeting the endogenous T locus with T2A-mKO2. ES cells were routinely maintained on gelatine-coated plates (Sigma, cat. G1890) in N2B27 media (Stem Cells inc, SCS-SF-NB-02) supplemented with 1μM PD0325901 and 3μM Chir99021 (2i) without LIF, and passaged with Accutase (Millipore, SF006) every 2-3 days. For sorting experiments, cells were plated for 24hrs in 2i at $1.5x10^4$ cells/cm^2 before washing once with PBS and changing the media to N2B27. After 24-26hrs, cells were sorted by flow cytometry according to GFP levels into Rex1-positive (highest 15%) and Rex1-negative (lowest 15%) populations using a MoFlo sorter (Beckman Coulter, inc). For neural differentiation, cells were plated at $1.0x10^4$ cells/cm^2 on laminin-coated dishes (Sigma-Aldrich, L2020) in N2B27. Medium was changed every other day. Definitive endoderm induction was as described (Morrison et al., 2015). Lateral mesoderm differentiation was performed by plating $1.2x10^4$ cells/cm^2 cells in collagen coated plates (BD BioCoat, 354591) in batch tested 10% Serum medium (GMEM (Sigma-Aldrich, G5154), 10% FCS (Sigma-Aldrich), 1x NEAA (Life Technologies, 11140-050), 1mM sodium pyruvate (Life Technologies, 11360-070), 1mM L-Glutamine (Life Technologies, 25030-081)) (Nishikawa et al., 1998).

ActivinA 10ng/ml and Chir99021 3μM (Gsk3(i)) treatment of sorted fractions was carried out on fibronectin-coated plates (Millipore, FC010) at $1.5x10^4$ cells/cm^2. Nodal inhibitor experiments were carried out using A8-301 1μM (Alk(i), Tocris Bioscience, 2939) or DMSO (1:10000) as a carrier control.

Colony forming assays were conducted by plating 1000 cells per well in laminin-coated 6 well plates in 2i supplemented with 100U/ml LIF to maximise self-renewal potential (Wray et al., 2011). After 5 days, cells were stained using alkaline phosphatase kit (Sigma, cat. 86 R-1KT) and the number of colonies counted.

For transcription factor induction of PGCLC, the tri-cistronic Ap2g-T2A-Prdm14-P2A-Blimp1 fragment (APB1, kind gift from Toshihiro Kobayashi and Azim Surani) was cloned into phCMV*1-cHA-IRES-H2BBFP plasmid. pPyCAG-PBase, pPBCAG-rtTA-IN and phCMV*1-APB-IRES-H2BBFP were co-transfected into *RGd2* cells by TransIT-LT1 (Kinoshita et al., 2015). G418 selection (400 μg/ml) was started 48 hours after transfection and cells were replated at clonal density at 96 hours. For PGCLC induction, cells sorted at 24 hours for Rex1-GFP expression were plated at 3,000 cells per well in a 96 round-bottomed well plate with (Nakaki et al., 2013) in the presence or absence of 1μg/ml Doxycycline (Sigma-Aldrich). Cells were fed every other day. Aggregates collected on day 2 and 4 for RT-qPCR or fixed after 4 days in culture.

Flow cytometry analysis of fluorescent reporters

Cells were dissociated into a single cell suspension using Accutase and resuspended in PBS+5% FBS for analysis using a BD LSR Fortessa Analyser.

Immunohistochemistry

Samples were fixed with 4% PFA for 10min at room temperature (RT), permeabilsed and blocked for 2hrs with block buffer (PBS+0.03%TritonX+3% donkey serum). Cells were incubated overnight at 4 °C in block buffer with the following primary antibodies: Sox1 (Cell Signalling, 4194, 1:200), Oct4 (Santa Cruz, sc-5279 or sc-8628, 1:400),

Nanog (eBioscience, 14-5761-80, 1:200), Klf4 (Abcam, ab72543, 1:300), Tuj1 (R&D, MAB1195, 1:500), Foxa2 (Abcam, ab40874, 1:200), Sox17 (R&D, AF1924, 1:200), T (R&D, AF2085, 1:200), Esrrb (Perseus, PP-H6705-00, 1:300), mKO2 (Amalgaam-MBL, M168-3, 1:1000), Blimp1 (eBiosciences, 14-5963-82). After three washes with PBS+0.03%TritonX, cells were incubated with secondary antibodies (Life Technoligies, 1:1000) and DAPI in blocking buffer for 3hrs in the dark. After three washes with PBS+0.03%TritonX, cells were left in PBS before imaging. Images were acquired with Laica DMI3000 B inverted microscope and the fluorescence in single cells quantified using CellProfiler (Jones et al., 2008). The number of cells was normalised to the highest value obtained for a given biological replicate.

Immunostaining of surface markers for flow cytometry

Cells were dissociated with enzyme-free Cell Dissociation Buffer (Life Technologies, 13151-014) at 37 °C. Cells were resuspended with staining buffer (PBS+1% Rat serum) and incubated with directly conjugated antibodies for 30min at 4 °C in the dark. After three washes with staining buffer, cells were analysed on an LSR Fortessa (BD Bioscineces). Spherotech beads were used to quantify the number of cells. The following antibodies were used: Ecadherin-eFluo660 (eBioscience, 50-3249-82), Cxcr4 (BD Biosciences, 552967 or 558644), Flk1 (BD Biosciences, 562941).

Gene expression analysis

RNA isolation from cell populations was performed with RNAeasy kit (Qiagen). SuperScriptIII (Invitrogen) and oligo-dT primers were used to synthesise cDNA. TaqMan probes were used for *Pou5f1* (Oct4), *Sox2*, *Nanog*, Esrrb, *Zfp42* (Rex1), *Klf2*,

397 *Otx2*, *Fgf5*, *Pim2, Sox1* and *Dnmt3b*. UPL primers were used for *Pou3f1* (fw:
398 catttttcgtttcgttttaccc, rv:gagcgcagaccctctctg, probe:72), *Smad2*
399 (fw:aggacggttagatgagcttgag, rv: gtccccaaatttcagagcaa, probe:9), *Tdgf1* (fw:
400 gtttgaatttggacccgttg, rv:ggaaggcacaaactggaaag, probe:93), *Nodal* (fw:
401 ccaaccatgcctacatcca, rv:cacagcacgtggaaggaac, probe:40), *Lefty2* (fw:
402 cacaagttggtccgtttcg, rv:ggtacctcggggtcacaat, probe:78), *Zic1* (fw: ggtacctcggggtcacaat,
403 rv:cctcgaactcgcacttgaa, probe:7), *Pou3f3* (fw: tctgagaccgcccacaag, rv:
404 gagcggcagtcagcaaag, probe:22).
405
406 **Gene knockdown**
407 Qiagen FlexiTube siRNAs for *Nodal, Tdgf1, Smad2* and *Smad3* at a final concentration
408 of 20nM were used for gene knockdown. $1.5x10^4$ cells/cm^2 were transfected in 24 well
409 plates containing 500μl of medium 2i medium with 0.5μl Lipfectamine RNAiMAX (Life
410 Technologies, 13778075) for. After overnight incubation, cells were washed once with
411 PBS before transfer to N2B27. Efficiency of transfection was quantified by flow
412 cytometry on Rex1GFPd2 cells transfected overnight with siRNA against GFP. Gene
413 knockdown was quantified by RT-qPCR after overnight transfection.
414
415 **Immunoblotting**
416 Western blotting was performed using standard techniques. The following primary
417 antibodies were used: Smad2 (Cell Signalling 3101, 1:1000 in 1% milk), p-Smad2 (Cell
418 Signalling, 3103, 1:1000 in 1% milk), anti-GAPDH (Sigma-Aldrich, G8795, 1:5000 in 1%
419 milk). Peroxidase-conjugated secondary antibodies were used (Sigma-Aldrich, 1:5000).

Amersham ECL Western Blotting detection reagent (RPN2106) was used according to manufacturers instructions.

Statistics

ANOVA was used to compare three or more samples. Two-tailed Student's t test was used for pairwise comparisons. Kolmogorov-Smirnov test was used to determine statistical significance of endoderm differentiation mixing experiments.

AUTHOR CONTRIBUTIONS

C.M., T.K. and A.S. designed the experiments. C.M. performed the experiments, analysed the data and prepared figures. A.S. supervised the study. C.M. and A.S. wrote the paper.

ACKNOWLEDGEMENTS

We thank Andy Riddell and Nigel Miller for flow cytometry and FACS support and Peter Humphreys for imaging support. We also thank Martin Leeb for creating and validating the TmKO2 reporter and Masaki Kinoshita for targeting and validated the *Rex1::GFPd2* APB1 cell line. The APB1 construct was a kind gift from Toshihiro Kobayashi and Azim Surani. We thank Jennifer Nichols, Kevin Chalut, Graziano Martello and Harry Leitch for discussions and comments on the manuscript. This research was funded by the Wellcome Trust. The Cambridge Stem Cell Institute receives core support from the Wellcome Trust and the Medical Research Council. C.M. was funded by a BBSRC studentship. A.S. is a Medical Research Council Professor.

REFERENCES

Arnold, S.J., Robertson, E.J., 2009. Making a commitment: cell lineage allocation and axis patterning in the early mouse embryo. Nat Rev Mol Cell Biol 10, 91–103. doi:10.1038/nrm2618

Beck, S., Le Good, J.A., Guzman, M., Haim, N.B., Roy, K., Beermann, F., Constam, D.B., 2002. Extraembryonic proteases regulate Nodal signalling during gastrulation. Nat Cell Biol 4, 981–985. doi:10.1038/ncb890

Beddington, R., Robertson, E.J., 1998. Anterior patterning in mouse. Trends in Genetics.

Bertero, A., Madrigal, P., Galli, A., Hubner, N.C., Moreno, I., Burks, D., Brown, S., Pedersen, R.A., Gaffney, D., Mendjan, S., Pauklin, S., Vallier, L., 2015. Activin/Nodal signaling and NANOG orchestrate human embryonic stem cell fate decisions by controlling the H3K4me3 chromatin mark. Genes Dev 29, 702–717. doi:10.1101/gad.255984.114

Betschinger, J., Nichols, J., Dietmann, S., Corrin, P.D., Paddison, P.J., Smith, A., 2013. Exit from pluripotency is gated by intracellular redistribution of the bHLH transcription factor Tfe3. Cell 153, 335–347. doi:10.1016/j.cell.2013.03.012

Boroviak, T., Loos, R., Bertone, P., Smith, A., Nichols, J., 2014. The ability of inner-cell-mass cells to self-renew as embryonic stem cells is acquired following epiblast specification. Nat Cell Biol. doi:10.1038/ncb2965

Boroviak, T., Loos, R., Lombard, P., Okahara, J., Behr, R., Sasaki, E., Nichols, J., Smith, A., Bertone, P., 2015. Lineage-Specific Profiling Delineates the Emergence and Progression of Naive Pluripotency in Mammalian Embryogenesis. Developmental Cell 35, 366–382. doi:10.1016/j.devcel.2015.10.011

Brennan, J., Lu, C.C., Norris, D.P., Rodriguez, T.A., Beddington, R.S., Robertson, E.J., 2001. Nodal signalling in the epiblast patterns the early mouse embryo. Nature 411, 965–969. doi:10.1038/35082103

Buecker, C., Srinivasan, R., Wu, Z., Calo, E., Acampora, D., Faial, T., Simeone, A., Tan, M., Swigut, T., Wysocka, J., 2014. Reorganization of Enhancer Patterns in Transition from Naive to Primed Pluripotency. Stem Cell 14, 838–853. doi:10.1016/j.stem.2014.04.003

Burtscher, I., Lickert, H., 2009. Foxa2 regulates polarity and epithelialization in the endoderm germ layer of the mouse embryo. Development 136, 1029–1038. doi:10.1242/dev.028415

Camus, A., Perea-Gomez, A., Moreau, A., Collignon, J., 2006. Absence of Nodal signaling promotes precocious neural differentiation in the mouse embryo. Dev Biol 295, 743–755. doi:10.1016/j.ydbio.2006.03.047

Choi, H.W., Joo, J.Y., Hong, Y.J., Kim, J.S., Song, H., Lee, J.W., Wu, G., Schöler, H.R., Do, J.T., 2016. Distinct Enhancer Activity of Oct4 in Naive and Primed Mouse Pluripotency. Stem Cell Reports 7, 911–926. doi:10.1016/j.stemcr.2016.09.012

Conlon, F.L., Barth, K.S., Robertson, E.J., 1991. A novel retrovirally induced embryonic lethal mutation in the mouse: assessment of the developmental fate of embryonic stem cells homozygous for the 413.d proviral integration. Development 111, 969–981.

Conlon, F.L., Lyons, K.M., Takaesu, N., Barth, K.S., Kispert, A., Herrmann, B.,

Robertson, E.J., 1994. A primary requirement for nodal in the formation and maintenance of the primitive streak in the mouse. Development 120, 1919–1928.

Dunn, S.-J., Martello, G., Yordanov, B., Emmott, S., Smith, A.G., 2014. Defining an essential transcription factor program for naïve pluripotency. Science 344, 1156–1160. doi:10.1126/science.1248882

Fiorenzano, A., Pascale, E., Aniello, C.D.A., Acampora, D., Bassalert, C., Russo, F., Andolfi, G., Biffoni, M., Francescangeli, F., Zeuner, A., Angelini, C., Chazaud, C., Patriarca, E.J., Fico, A., Minchiotti, G., 2016. Cripto is essential to capture mouse epiblast stem cell and human embryonic stem cell pluripotency. Nature Communications 7, 1–16. doi:10.1038/ncomms12589

Gadue, P., Huber, T.L., Paddison, P.J., Keller, G.M., 2006. Wnt and TGF-beta signaling are required for the induction of an in vitro model of primitive streak formation using embryonic stem cells. Proc Natl Acad Sci USA 103, 16806–16811. doi:10.1073/pnas.0603916103

Gardner, R.L., 1975. Analysis of determination and differentiation in the early mammalian embryo using intra- and interspecific chimeras. Symp Soc Dev Biol 207–236.

Guzman-Ayala, M., Ben-Haim, N., Beck, S., Constam, D.B., 2004. Nodal protein processing and fibroblast growth factor 4 synergize to maintain a trophoblast stem cell microenvironment. Proc Natl Acad Sci USA 101, 15656–15660. doi:10.1073/pnas.0405429101

Habibi, E., Brinkman, A.B., Arand, J., Kroeze, L.I., Kerstens, H.H.D., Matarese, F., Lepikhov, K., Gut, M., Brun-Heath, I., Hubner, N.C., Benedetti, R., Altucci, L., Jansen, J.H., Walter, J., Gut, I.G., Marks, H., Stunnenberg, H.G., 2013. Whole-genome bisulfite sequencing of two distinct interconvertible DNA methylomes of mouse embryonic stem cells. Cell Stem Cell 13, 360–369. doi:10.1016/j.stem.2013.06.002

Hayashi, K., Ohta, H., Kurimoto, K., Aramaki, S., Saitou, M., 2011. Reconstitution of the mouse germ cell specification pathway in culture by pluripotent stem cells. Cell 146, 519–532. doi:10.1016/j.cell.2011.06.052

Jones, T.R., Kang, I.H., Wheeler, D.B., Lindquist, R.A., Papallo, A., Sabatini, D.M., Golland, P., Carpenter, A.E., 2008. CellProfiler Analyst: data exploration and analysis software for complex image-based screens. BMC Bioinformatics. doi:10.1186/1471-2105-9-482

Kalkan, T., Olova, N., Roode, M., Mulas, C., Lee, H.J., Nett, I., Marks, H., Walker, R., Stunnenberg, H.G., Lilley, K., Nichols, J., Reik, W., Bertone, P., Smith, A., 2016. Tracking the embryonic stem cell transition from ground state pluripotency 1–31. doi:10.1101/092510

Kalkan, T., Smith, A., 2014. Mapping the route from naive pluripotency to lineage specification. Philosophical Transactions of the Royal Society B: Biological Sciences 369. doi:10.1098/rstb.2013.0540

Kinoshita, M., Shimosato, D., Yamane, M., Niwa, H., 2015. Sox7 is dispensable for primitive endoderm differentiation from mouse ES cells. BMC Dev Biol 15, 1. doi:10.1186/s12861-015-0079-4

Kunath, T., Saba-El-Leil, M.K., Almousailleakh, M., Wray, J., Meloche, S., Smith, A., 2007. FGF stimulation of the Erk1/2 signalling cascade triggers transition of pluripotent embryonic stem cells from self-renewal to lineage commitment. Development 134, 2895–2902. doi:10.1242/dev.02880

537 Kurimoto, K., Yabuta, Y., Ohinata, Y., Shigeta, M., Yamanaka, K., Saitou, M., 2008.
538 Complex genome-wide transcription dynamics orchestrated by Blimp1 for the
539 specification of the germ cell lineage in mice. Genes Dev 22, 1617–1635.
540 doi:10.1101/gad.1649908
541 Lee, M.K., Tuttle, J.B., Rebhun, L.I., Cleveland, D.W., Frankfurter, A., 1990. The
542 expression and posttranslational modification of a neuron-specific beta-tubulin
543 isotype during chick embryogenesis. Cell Motil. Cytoskeleton 17, 118–132.
544 doi:10.1002/cm.970170207
545 Leeb, M., Dietmann, S., Paramor, M., Niwa, H., Smith, A., 2014. Genetic exploration of
546 the exit from self-renewal using haploid embryonic stem cells. Cell Stem Cell 14,
547 385–393. doi:10.1016/j.stem.2013.12.008
548 Leitch, H.G., McEwen, K.R., Turp, A., Encheva, V., Carroll, T., Grabole, N., Mansfield,
549 W., Nashun, B., Knezovich, J.G., Smith, A., Surani, M.A., Hajkova, P., 2013. Naive
550 pluripotency is associated with global DNA hypomethylation. Nat Struct Mol Biol.
551 doi:10.1038/nsmb.2510
552 Lu, C.C., Robertson, E.J., 2004. Multiple roles for Nodal in the epiblast of the mouse
553 embryo in the establishment of anterior-posterior patterning. Developmental Biology
554 273, 149–159. doi:10.1016/j.ydbio.2004.06.004
555 Magnúsdóttir, E., Dietmann, S., Murakami, K., Günesdogan, U., Tang, F., Bao, S.,
556 Diamanti, E., Lao, K., Göttgens, B., Azim Surani, M., 2013. A tripartite transcription
557 factor network regulates primordial germ cell specification in mice. Nat Cell Biol 15,
558 905–915. doi:10.1038/ncb2798
559 Magnúsdóttir, E., Gillich, A., Grabole, N., Surani, M.A., 2012. Combinatorial control of
560 cell fate and reprogramming in the mammalian germline. Curr Opin Genet Dev 22,
561 466–474. doi:10.1016/j.gde.2012.06.002
562 Marks, H., Kalkan, T., Menafra, R., Denissov, S., Jones, K., Hofemeister, H., Nichols, J.,
563 Kranz, A., Stewart, A.F., Smith, A., Stunnenberg, H.G., 2012. The Transcriptional
564 and Epigenomic Foundations of Ground State Pluripotency. Cell 149, 590–604.
565 doi:10.1016/j.cell.2012.03.026
566 Martello, G., Smith, A., 2014. The nature of embryonic stem cells. Annu Rev Cell Dev
567 Biol 30, 647–675. doi:10.1146/annurev-cellbio-100913-013116
568 Matulka, K., Lin, H.H., Hříbková, H., Uwanogho, D., Dvořák, P., 2013. PTP1B Is an
569 Effector of Activin Signaling and Regulates Neural Specification of Embryonic Stem
570 Cells. Cell Stem Cell.
571 Mesnard, D., Donnison, M., Fuerer, C., Pfeffer, P.L., Constam, D.B., 2011. The
572 microenvironment patterns the pluripotent mouse epiblast through paracrine Furin
573 and Pace4 proteolytic activities. Genes Dev 25, 1871–1880.
574 doi:10.1101/gad.16738711
575 Mesnard, D., Guzman-Ayala, M., Constam, D.B., 2006. Nodal specifies embryonic
576 visceral endoderm and sustains pluripotent cells in the epiblast before overt axial
577 patterning. Development 133, 2497–2505. doi:10.1242/dev.02413
578 Morrison, G., Scognamiglio, R., Trumpp, A., Smith, A., 2015. Convergence of cMyc
579 and -catenin on Tcf7l1 enables endoderm specification. EMBO J 1–13.
580 doi:10.15252/embj.201592116
581 Morrison, G.M., Oikonomopoulou, I., Migueles, R.P., Soneji, S., Livigni, A., Enver, T.,
582 Brickman, J.M., 2008. Anterior definitive endoderm from ESCs reveals a role for
583 FGF signaling. Cell Stem Cell 3, 402–415. doi:10.1016/j.stem.2008.07.021
584 Mullen, A.C., Orlando, D.A., Newman, J.J., Lovén, J., Kumar, R.M., Bilodeau, S.,

585 Reddy, J., Guenther, M.G., DeKoter, R.P., Young, R.A., 2011. Master transcription
586 factors determine cell-type-specific responses to TGF-β signaling. Cell 147, 565–
587 576. doi:10.1016/j.cell.2011.08.050
588 Nakaki, F., Hayashi, K., Ohta, H., Kurimoto, K., Yabuta, Y., Saitou, M., 2013. Induction
589 of mouse germ-cell fate by transcription factors in vitro. Nature 501, 222–226.
590 doi:10.1038/nature12417
591 Nichols, J., Smith, A., 2012. Pluripotency in the embryo and in culture. Cold Spring
592 Harbor Perspectives in Biology 4, a008128–a008128.
593 doi:10.1101/cshperspect.a008128
594 Nishikawa, S.I., Nishikawa, S., Hirashima, M., Matsuyoshi, N., Kodama, H., 1998.
595 Progressive lineage analysis by cell sorting and culture identifies FLK1+VE-
596 cadherin+ cells at a diverging point of endothelial and hemopoietic lineages.
597 Development 125, 1747–1757.
598 Niwa, H., Yamamura, K., Miyazaki, J., 1991. Efficient selection for high-expression
599 transfectants with a novel eukaryotic vector. Gene 108, 193–199. doi:10.1016/0378-
600 1119(91)90434-D
601 Ogawa, K., Matsui, H., Ohtsuka, S., Niwa, H., 2004. A novel mechanism for regulating
602 clonal propagation of mouse ES cells. Genes to Cells 9, 471–477.
603 doi:10.1111/j.1356-9597.2004.00736.x
604 Ogawa, K., Saito, A., Matsui, H., Suzuki, H., Ohtsuka, S., Shimosato, D., Morishita, Y.,
605 Watabe, T., Niwa, H., Miyazono, K., 2007. Activin-Nodal signaling is involved in
606 propagation of mouse embryonic stem cells. J Cell Sci 120, 55–65.
607 doi:10.1242/jcs.03296
608 Peng, G., Suo, S., Chen, J., Chen, W., Liu, C., Yu, F., Wang, R., Chen, S., Sun, N., Cui,
609 G., Song, L., Tam, P.P.L., Han, J.-D.J., Jing, N., 2016. Spatial Transcriptome for the
610 Molecular Annotation of Lineage Fates and Cell Identity in Mid-gastrula Mouse
611 Embryo. Developmental Cell 36, 681–697. doi:10.1016/j.devcel.2016.02.020
612 Pevny, L.H., Sockanathan, S., Placzek, M., Lovell-Badge, R., 1998. A role for SOX1 in
613 neural determination. Development 125, 1967–1978.
614 Robertson, E.J., 2014. Dose-dependent Nodal/Smad signals pattern the early mouse
615 embryo. Seminars in cell & developmental biology.
616 Rossant, J., 1975. Investigation of the determinative state of the mouse inner cell mass.
617 Development 33, 979–990.
618 Rossant, J., Tam, P., 2009. Blastocyst lineage formation, early embryonic asymmetries
619 and axis patterning in the mouse. Development 136, 701–713. doi:136/5/701 [pii]
620 10.1242/dev.017178
621 Smith, A.G., *in press*. Formative pluripotency: the executive phase in a developmental
622 continuum.
623 Stavridis, M.P., Lunn, J.S., Collins, B.J., Storey, K.G., 2007. A discrete period of FGF-
624 induced Erk1/2 signalling is required for vertebrate neural specification.
625 Development 134, 2889–2894. doi:10.1242/dev.02858
626 Thomas, P., Beddington, R., 1996. Anterior primitive endoderm may be responsible for
627 patterning the anterior neural plate in the mouse embryo. Current Biology 6, 1487–
628 1496.
629 Tojo, M., Hamashima, Y., Hanyu, A., Kajimoto, T., Saitoh, M., Miyazono, K., Node, M.,
630 Imamura, T., 2005. The ALK-5 inhibitor A-83-01 inhibits Smad signaling and
631 epithelial-to-mesenchymal transition by transforming growth factor-beta. Cancer Sci.
632 96, 791–800. doi:10.1111/j.1349-7006.2005.00103.x

633 Toyooka, Y., Shimosato, D., Murakami, K., Takahashi, K., Niwa, H., 2008. Identification
634 and characterization of subpopulations in undifferentiated ES cell culture.
635 Development 135, 909–918. doi:135/5/909 [pii]
636 10.1242/dev.017400
637 Tsakiridis, A., Huang, Y., Blin, G., Skylaki, S., Wymeersch, F., Osorno, R., Economou,
638 C., Karagianni, E., Zhao, S., Lowell, S., Wilson, V., 2014. Distinct Wnt-driven
639 primitive streak-like populations reflect in vivo lineage precursors. Development 141,
640 1209–1221. doi:10.1242/dev.101014
641 Turner, D.A., Trott, J., Hayward, P., Rué, P., Martinez Arias, A., 2014. An interplay
642 between extracellular signalling and the dynamics of the exit from pluripotency
643 drives cell fate decisions in mouse ES cells. Biology Open 3, 614–626.
644 doi:10.1242/bio.20148409
645 Wray, J., Kalkan, T., Gomez-Lopez, S., Eckardt, D., Cook, A., Kemler, R., Smith, A.,
646 2011. Inhibition of glycogen synthase kinase-3 alleviates Tcf3 repression of the
647 pluripotency network and increases embryonic stem cell resistance to differentiation.
648 Nat Cell Biol 13, –845. doi:10.1038/ncb2267
649 Wray, J., Kalkan, T., Smith, A., 2010. The ground state of pluripotency. Biochem Soc
650 Trans 38, 1027–1032. doi:BST0381027 [pii]
651 10.1042/BST0381027
652 Yamashita, J., Itoh, H., Hirashima, M., Ogawa, M., Nishikawa, S., Yurugi, T., Naito, M.,
653 Nakao, K., 2000. Flk1-positive cells derived from embryonic stem cells serve as
654 vascular progenitors. Nature 408, 92–96. doi:10.1038/35040568
655 Yang, S.-H., Kalkan, T., Morrisroe, C., Smith, A., Sharrocks, A.D., 2012. A genome-wide
656 RNAi screen reveals MAP kinase phosphatases as key ERK pathway regulators
657 during embryonic stem cell differentiation. PLoS Genet 8, e1003112.
658 doi:10.1371/journal.pgen.1003112
659 Yasunaga, M., Tada, S., Torikai-Nishikawa, S., Nakano, Y., Okada, M., Jakt, L.M.,
660 Nishikawa, S., Chiba, T., Era, T., Nishikawa, S.-I., 2005. Induction and monitoring of
661 definitive and visceral endoderm differentiation of mouse ES cells. Nat Biotechnol
662 23, 1542–1550. doi:10.1038/nbt1167
663 Ying, Q., Wray, J., Nichols, J., Batlle-Morera, L., Doble, B., Woodgett, J., Cohen, P.,
664 Smith, A., 2008. The ground state of embryonic stem cell self-renewal. Nature 453,
665 519–523. doi:nature06968 [pii]
666 10.1038/nature06968
667 Ying, Q.-L., Stavridis, M., Griffiths, D., Li, M., Smith, A., 2003. Conversion of embryonic
668 stem cells into neuroectodermal precursors in adherent monoculture., Nature
669 biotechnology. doi:10.1038/nbt780
670 Zhang, K., Li, L., Huang, C., Shen, C., Tan, F., Xia, C., Liu, P., Rossant, J., Jing, N.,
671 2010. Distinct functions of BMP4 during different stages of mouse ES cell neural
672 commitment. Development 137, 2095–2105. doi:10.1242/dev.049494
673 Zhou, X., Sasaki, H., Lowe, L., Hogan, B.L., Kuehn, M.R., 1993. Nodal is a novel TGF-
674 beta-like gene expressed in the mouse node during gastrulation. Nature 361, 543–
675 547. doi:10.1038/361543a0
676 Zylicz, J.J., Dietmann, S., Günesdogan, U., Hackett, J.A., 2015. Chromatin dynamics
677 and the role of G9a in gene regulation and enhancer silencing during early mouse
678 development. eLife. doi:10.7554/eLife.09571.001
679
680

FIGURE LEGENDS

Figure 1. Acquisition of PGC-LC differentiation capacity

(**A**) Experimental set up for transcription-factor dependent PGC-like cell specification.

(**B**) Expression of Blimp1 and Oct4 in day 4 aggregates differentiated in the presence or absence of Dox to induce transcription factor overexpression. Scale bar: 60μm

(**C**) Zoom in of the expression of Blimp1 and Oct4 in day 4 aggregates differentiated in the presence or absence of Dox to induce transcription factor overexpression. Arrow heads show overexpression artefacts. Scale bar: 20μm

(**D**) Quantification of the Blimp1 staining on day 4 in aggregates after addition of Dox.

(**E**) RT-qPCR of endogenous PGC-associated transcripts.

Mean and SD for 2 independent experiments shown, *p<0.01, **p<0.001 (Student t test).

See also Figure S1

Figure 2. Multilineage differentiation capacity is manifest in Rex1-negative cells

(**A**) Experimental set up and sample analysis for ActivinA+GSK3(i) treatment. Histogram shows the percentages of cells expressing *T:mKO2* or *RGd2* (**B**).

(**C**) Experimental set up and sample analysis for lateral mesoderm differentiation. Histogram showing the percentage of Flk1+/Ecadh- cells.

(**D**) Experimental set up and sample analysis for definitive endoderm differentiation.

(**E**) Percentage of Cxcr4+/Ecadh+ double positive cells.

(**F**) Normalised number of cells during definitive endoderm differentiation. The number of cells was normalised to the highest value obtained in that biological replicate.

(**G**) Single cell analysis during definitive endoderm differentiation by seeding fluorescently labelled Rex1-High or Rex1-Low cells at clonal density amongst unlabelled cells.

(**H**) Number of clones after 4 days of differentiation.

(**I**) Histogram showing the distribution of the percentage of Sox17 positive cells per clone. Two independent experiments, all data shown.

(**J**) Histogram showing the distribution of the number of cells per clone. Two independent experiments, all data shown.

(**K**) Experimental set up and sample analysis for neural differentiation. Histogram showing the percentage of Sox1-positive cells during the differentiation time-course.

Unless stated, mean and SD for 3 independent experiments shown, * $p<0.05$, ** $p<0.01$. See also Figure S2.

Figure 3. Inhibition of endogenous Nodal signalling does not affect exit from the naïve state

(**A**) Experimental set up

(**B**) Relative expression of pluripotency factors *Klf2* and *Nanog* over time when cells are differentiated in DMSO or Alk(i).

(**C**) Percentage of Klf4 and Nanog positive cells over time after 2i withdrawal when cells are differentiate in the presence of DMSO or Alk(i).

(**D**) Self-renewal capacity declines at a comparable rate for cells treated with DMSO vehicle or Alk(i).

(**E**) Relative expression of post-implantation markers *Fgf5* and *Otx2* shows faster earlier downregulated for cells treated with Alk(i) over DMSO controls.

(**F**) Relative expression of neural-associated genes *Sox1, Zic1* and *Pou3f3* over time when cells are differentiated in DMSO or Alk(i).

(**G**) Inhibition of Nodal signalling results in accelerated reduction of Oct4 protein and increase in Sox1 protein at day 3 of differentiation.

Mean and SD for 2 independent experiments shown. See also Figure S3.

Figure 4. Nodal signalling during exit from the naïve state prevents preconscious neutralisation.

(**A**) Inhibition of Nodal signalling with Alki(i) in Rex1-positive and Rex1-negative sorted fractions. Graphs show percentage of Sox1 positive cells after sort.

(**B**) Percentage of Sox1 positive cells arising from Rex1-negative cells following DMSO (control) or Alk(i) treatment.

(**C**) Number of cells over the period analysed in B.

(**D**) ActivinA/Gsk3(i) induction of Alk(i) or control treated Rex1-negative cells. Numbers of TmKO2 positive cells, along with total cell numbers (**E**).

To determine the normalised number of cells as a percentage for each biological replicate, the number of cells was normalised by the highest value obtained in that biological replicate.

(**F**) Experimental set up of definitive endoderm clonal assay.

(**G**) Histogram showing the distribution of the percentage of Sox17 positive cells per clone. Two independent experiments, all data shown.

(**H**) Histogram showing the distribution of the number of cells per clone. Two independent experiments, all data shown.

Unless states, mean and SD for 3 independent experiments shown, * $p<0.05$, ** $p<0.01$.

(**I**) Experimental set up of transcription-factor dependent PGC-LC differentiation. Images show day 4 cultures in the presence of Dox from Alk(i)-treated and control cells. Scale bar=1mm.

(**J**) RT-qPCR of PGC-associated genes during induction process. Mean and SD for 2 independent experiments shown, *$p<0.05$, $p<001$. See also Figure S4.

SUPPLEMENTARY FIGURE LEGENDS

Figure S1

(**A**) Flow cytometry histogram of RGd2 cells after removal of 2i.

(**B**) Experimental set up for sorting experiments.

(**C**) Flow cytometry profile of sorted fractions

(**D**) Replating capacity of 2i, 24hrs Rex1-positive and 24hrs Rex1-negative cells in 2i/LIF media.

(**E**) Replating capacity of 2i, 24hrs Rex1-positive and 24hrs Rex1-negative cells in Serum/Lif media.

(**F**) Quantification of Oct4 immunostaining in day 4 aggregates in the presence of Dox. Mean and SD for 3 independent experiments shown.

Figure S2

(**A**) Flow cytometry plots of Rex1GFPd2+TmKO2 cells in 2i, and Rex1-positive sorted cells for 3 days in control or ActivinA+GSK3(i).

774 (**B**) Percentage of cells staining positive for Sox17 and Foxa2 during definitive
775 endoderm differentiation.
776 (**C**) Normalised number of cells during neural differentiation.
777 (**D**) Immunostaining for Sox1 and Tuj1 of 2i, Rex1-positive and Rex1-negative cells after
778 6 and 8 days of differentiation.
779 To determine the normalised number of cells as a percentage for each biological
780 replicate, the number of cells was normalised by the highest value obtained in that
781 biological replicate.
782 Mean and SD for three independent experiments shown.
783
784 **Figure S3**
785 (**A**) Western blot showing p-Smad2, Smad2 and Gapdh protein in cells treated with
786 control or Alk(i) for 30min.
787 (**B**) Number of colonies of ES cells grown in 2i+DMSO or 2i+Alk(i) for three passages.
788 Mean and SD for two independent experiments is shown.
789 (**C**) RT-qPCR of *Nodal*, *Tdgf1* and *Smad2/3* siRNA treated cells after overnight
790 transfection in 2i. siRNA knockdown did not affect the expression of pluripotency genes
791 *Pou5f1, Klf4* or *Nanog* but in some cases it did affect the expression of the Nodal
792 signalling target *Lefty2.*
793 (**D**) Quantification of the number of Oct4/Sox2 double positive cells, Oct4 negative/Sox2
794 positive and Sox2/Sox1 double positive cells on day 3 of neural differentiation after
795 treatment with siRNA. Mean and SD for two independent experiments is shown. * $p < 0.05$, ** $p < 0.01$
796
797

Figure S4

(**A**) Expression of Nodal pathway signalling components in 2i, Rex1-positive and Rex1-negative cells (Kalkan et al.).

(**B**) Nodal inhibition before and during downregulation of Rex1 – Flow cytometry plot of Rex1GFPd2 cells differentiated for 24hrs in Alk(i) or control (DMSO).

(**C**) Relative expression of pluripotency and differentiation factors in Rex1-negative cells arising from control or Alk(i) conditions by RT-qPCR. 2i and Rex1-positive cells are included as controls.

(**D**) Expression of *Sox1* in the sorted fractions.

(**E**) Percentage of TmKO2 positive cells during ActivinA/Gsk3(i) treatment of Control or Alk(i) derived Rex1-negative cells. Mean and SD for 3 independent experiments shown, *$p<0.05$.

(**F**) Lateral mesoderm differentiation of 24hrs Alk(i) or control treated Rex1-negaive cells.

(**G**) Percentage of Flk1+/Ecadh- cells.

(**H**) Histogram showing the normalised number of cells.

(**I**) Number of clones after 4 days of definitive endoderm differentiation.

To determine the normalised number of cells as a percentage for each biological replicate, the number of cells was normalised by the highest value obtained in that biological replicate. Mean and SD for 3 independent experiments shown, *$p<0.05$.

Figure 1

A Transcription factor-dependent PGC-like cell induction

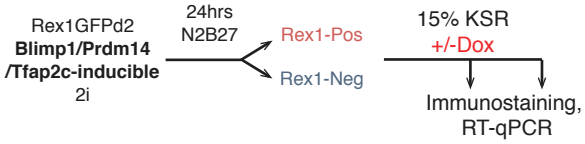

B

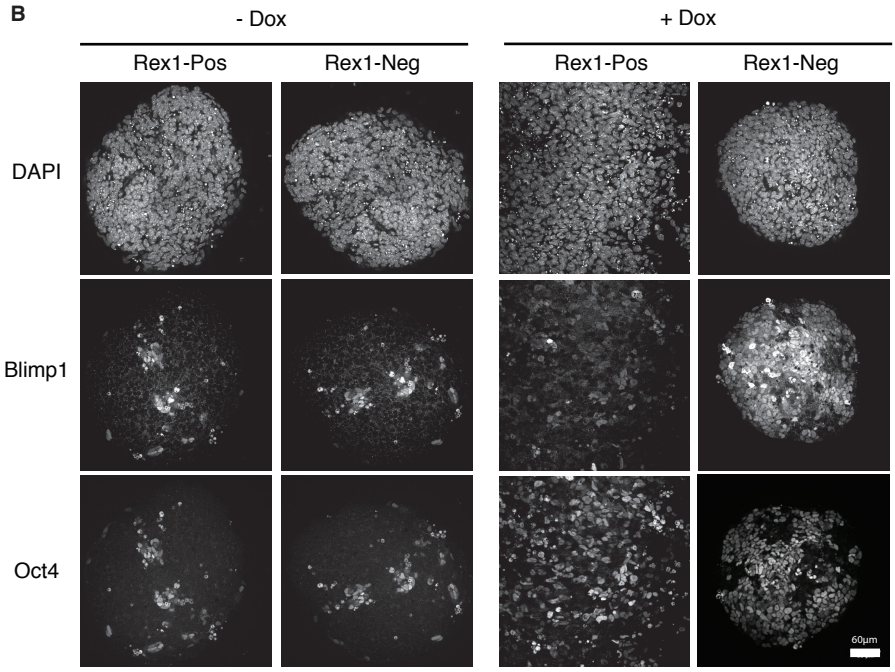

C

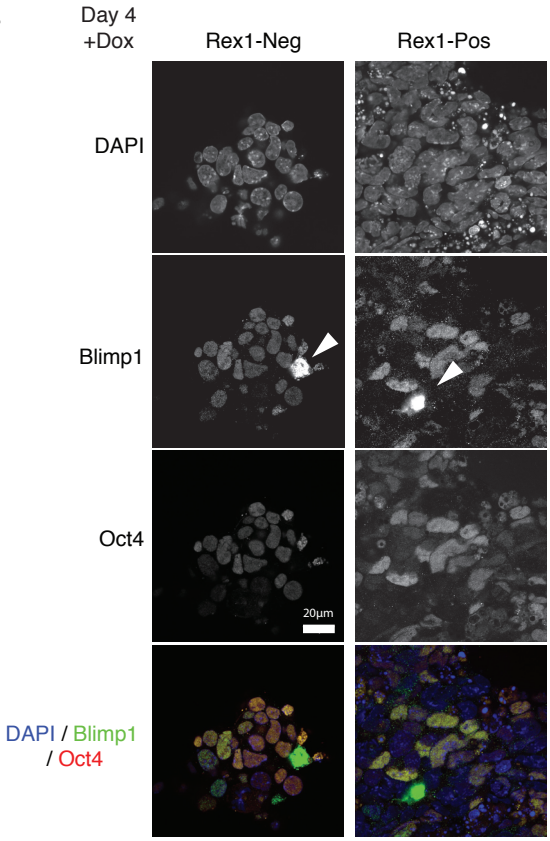

D

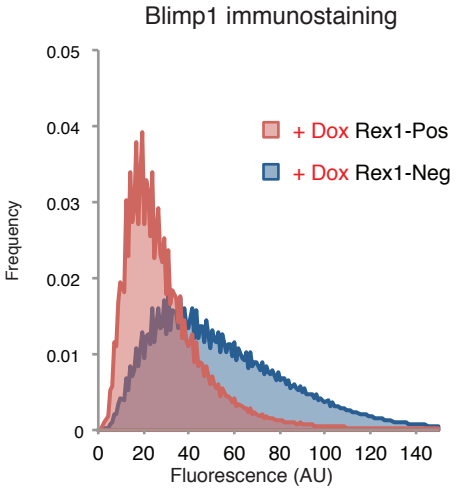

E

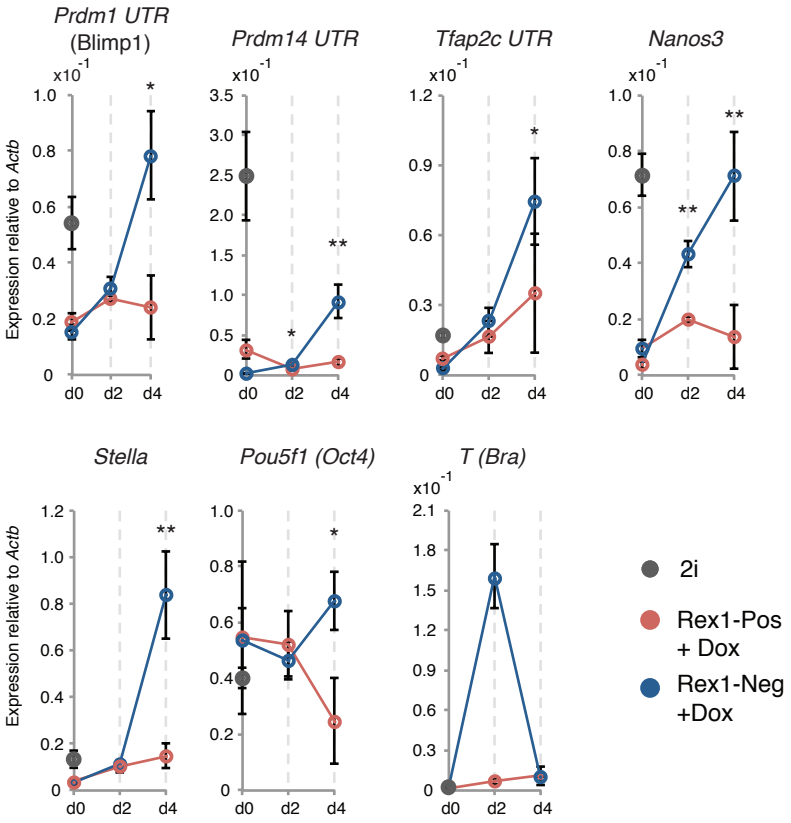

Figure 2

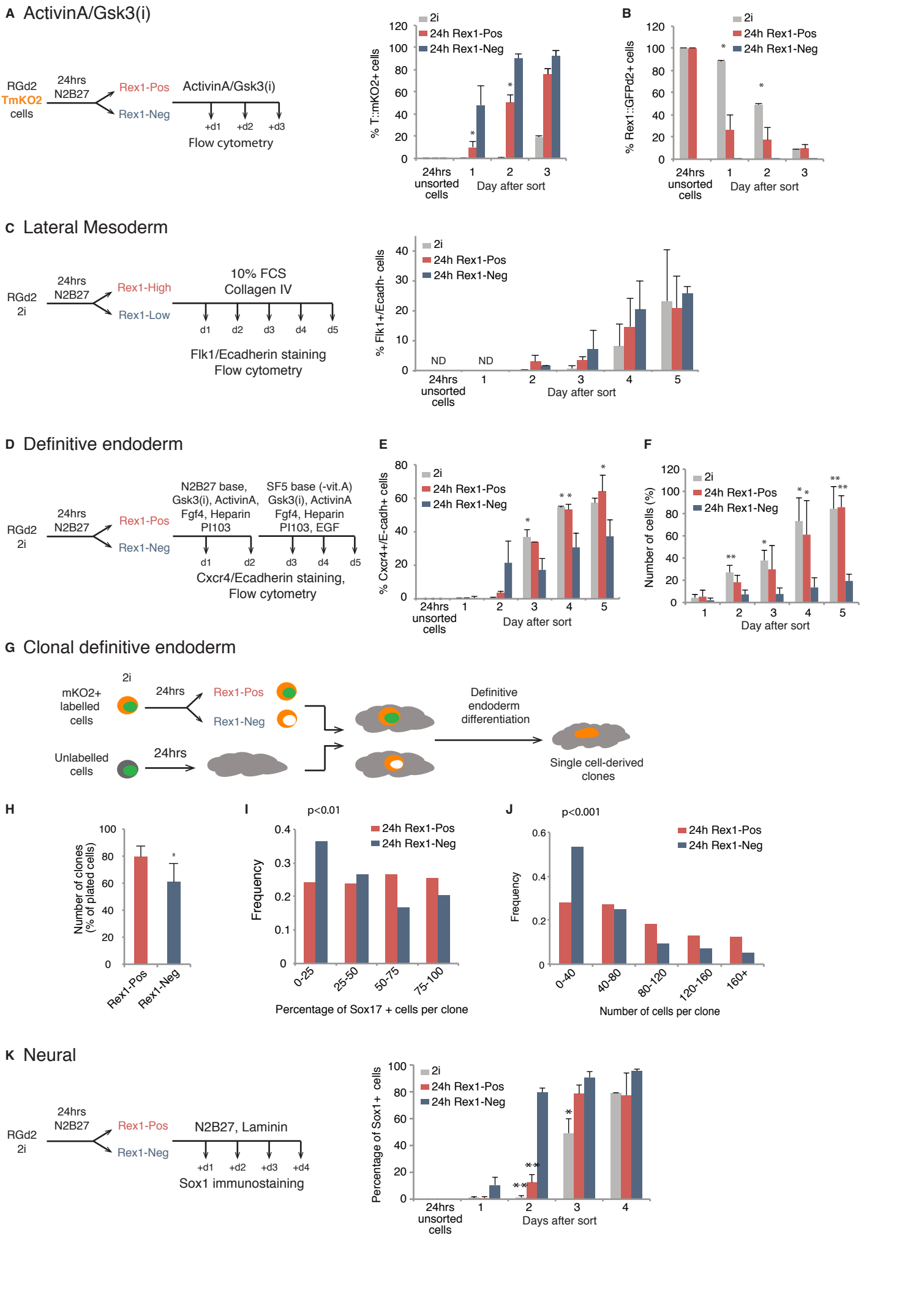

Figure 3

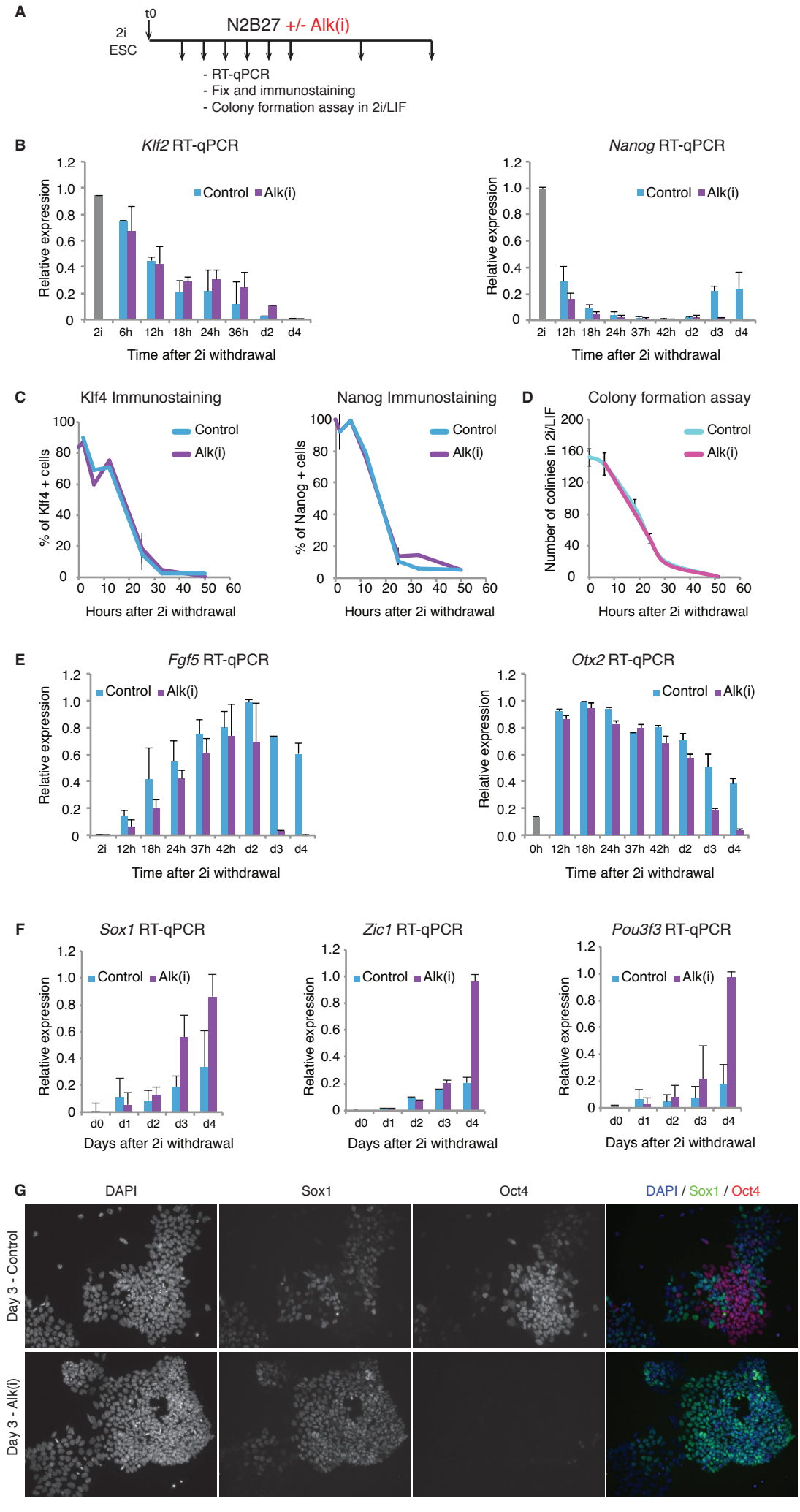

Figure 4

Nodal inhibition after Rex1 downregulation

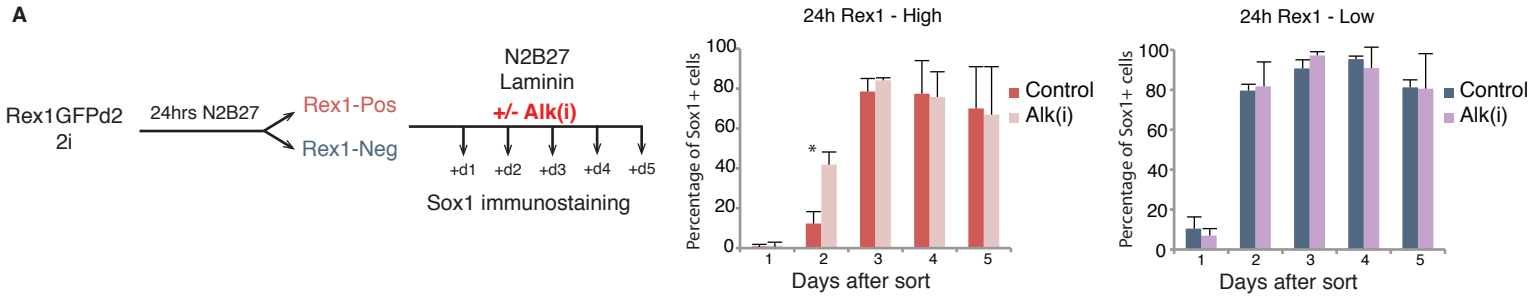

Nodal inhibition before and during Rex1 downregulation